Korean J. Chem. Eng., **24**(4), 679-682 (2007)

SHORT COMMUNICATION

Effect of framework or textural nanoporosity on the bulk morphology of mesoporous aluminas

Younghun Kim†, Byunghwan Lee* and Jongheop Yi**

Department of Chemical Engineering, Kwangwoon University, Wolgye-dong, Nowon-gu, Seoul 139-701, Korea
*Department of Chemical System Engineering, Keimyung University, Sindang-dong, Dalseo-gu, Daegu 704-701, Korea
**School of Chemical and Biological Engineering, Seoul National University, Shillim-dong, Gwanak-gu, Seoul 151-742, Korea
(*Received 3 November 2006 • accepted 16 January 2007*)

Abstract–The framework and/or textural porosity of mesoporous aluminas (MA), which have great potential for use in applications such as adsorbents and catalytic supports, is dependent on the conditions used in their preparation. The nanoporosity of MA affects their adsorption capacity and catalytic activity, and the bulk morphology of an MA is related to the development of the framework and/or textural porosity. An MA with a well-developed framework pore was found to have a smooth surface, while an MA with a well-developed textural pore had a coarse and aggregated morphology.

Key words: Nanoporosity, Mesoporous Alumina, Morphology

INTODUCTION

The specific features of mesoporous materials, which have a high surface area, large pore volume, narrow pore size distribution and uniform pore structure, indicate their high potential for use as ideal adsorbents and catalytic supports. For example, mesoporous aluminas (MA) show high uptake capacities for heavy metal ions, organic dyes and arsenic from aqueous solutions [1,2] due to their large surface area. In addition, metal supported MA can be used as an efficient catalyst for hydrogenation, hydrodechlorination, and others, because of their thermal, chemical, and mechanical stability [3,4]. Tailor-made MA can be easily prepared by a post-hydrolysis method at ambient conditions [5-8], and Ni/Al_2O_3 with nanoporosity with nickel salts of stearic acid can be prepared in a one-step synthesis [9].

According to the polymerization behavior of metal alkoxides in an aqueous phase [10], primary particles grow by Ostwald ripening, and the final particles can be 1-20 μm in size. Primary particles, which have a framework pore induced by a template (e.g., stearic acid), are aggregated and then form a secondary pore (i.e., textural pore) in the void between one and other particles. Framework and textural pores have an effect on adsorption capacity and catalytic efficiency [11]. The former serves as support for the active sites for adsorption and catalytic reactions, and occupy most of the surface area. The latter might enhance the accessibility of target materials to inner framework pores, but show an irregular pore structure. Mercier et al. [12] reported that in an amorphous silica gel to which ligands had been grafted, the narrow pore channels were blocked, thus creating a bottleneck. In contrast, the uniform pore morphology of a mesoporous molecular sieve leads to a grafted material in which the access of ions to all the functional sites is unrestricted. Kim and co-workers [11] reported that the mercapto concentration showed a low correlation with pore size and the surface area of the supports, but was strongly dependent on the framework pore volume.

The activity of MA is affected by the pore types, and it would be predicted that the bulk morphology of MA is correlated with its pore type. Namely, MA with well-developed framework pores might show a solid morphology. In this work, we investigated the effect of framework and/or textural nanoporosity on the bulk morphology of MAs.

EXPERIMENTAL

Water and *sec*-butyl alcohol were used as an initiator for condensation and as a surfactant solvent, respectively. The aluminum source and surfactant were separately dissolved in *sec*-butyl alcohol, and the two solutions were then mixed. Small amounts of water were slowly added dropwise to the mixture at rate of 1 ml/min, resulting in a white precipitate. The rest of the experimental procedure has been described elsewhere [5]. The molar ratio of this reaction mixture was 1 Al(*sec*-BuO)$_3$: 0.2 carboxylic acids : 0.04 NaOH : 5 *sec*-BuOH : 4-48 H_2O (within appropriate 1 M HNO_3).

N_2 adsorption/desorption experiments were carried out by using a Micromeritics ASAP 2010 analyzer. The surface morphology of the mesoporous alumina was examined by SEM (Model XL-20, Philips). The porosity of calcined samples was characterized by transmission electron microscopy (TEM) on a JEM-2000EXII. NMR spectra were obtained on a Varian-Inova spectrometer (300 MHz) at MAS frequency of 6 kHz.

RESULTS AND DISCUSSION

The surface morphologies of the prepared mesoporous aluminas were analyzed by SEM. As shown in Fig. 1, the morphology of MA was different with the preparation conditions employed. MA-1 (Fig. 1a) showed aggregated particles with a coarse surface which was composed of primary small particles, while MA-2 (Fig. 1b) revealed a solidified smooth surface. The particle size of MA-2 was also larger than that of MA-1. MA-3 (Fig. 1c) has features of both MA-1

†To whom correspondence should be addressed.
E-mail: korea1@kw.ac.kr

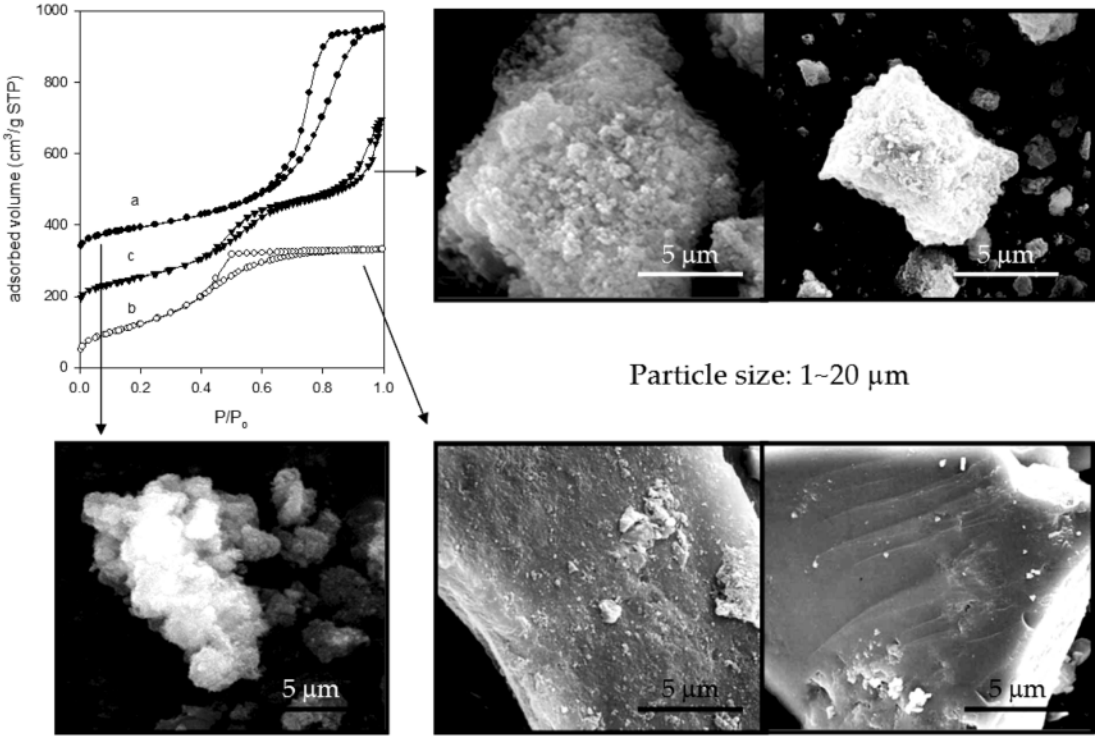

Fig. 1. SEM images and N2 adsorption/desorption isotherms of (a) MA-1 (well-developed textural porosity), (b) MA-2 (well-developed framework porosity), and (c) MA-3 (well-developed textural and framework porosity).

and MA-2, and, thus, showed a solidified coarse surface. The particle size of MA-3 was intermediate between MA-2 and MA-1. Similarly, SBA-16 [13] is a family of mesoporous silica, with a polyhedral or spherical shape, depending on the preparation conditions used, and MCM-41 [14] had a spherical or wedge shape.

As shown in the N_2 adsorption/desorption isotherms, mesoporous aluminas as well as mesoporous silicas might reveal a correlation between surface morphology and nanoporosities. The porosity of MA varied with the synthesis conditions used, and hysteresis curves were found near relative pressures 0.5 and/or 0.9. Tanev et al. [15] defined and classified these terms as framework porosity and textural porosity. Framework porosity represents the porosity contained within the uniform channels of a templated framework, while textural porosity represents porosity arising from non-crystalline intra-aggregate voids and spaces formed as a result of interparticle contact. MA-3 contains both framework and textural porosity. MA-1 with a coarse surface and MA-2 with a smooth surface display the well-developed textural (0.8-1.0 P/P_o) and framework (0.4-0.7 P/P_o) porosity in their N_2 isotherms, respectively. The textural porosity in MA-1 is present in most of the adsorbed volume, and thus a large pore size would be expected, compared to MA-2 and MA-3 with framework porosity as the main pore. Therefore, the N_2 isotherm and SEM results show that the bulk morphology of mesoporous alumina is correlated with nanoporosity.

This feature was similarly found in the case of MCM-41, reported by Grun and co-workers [14]. The relation between nanoporosity and surface morphology is also discussed in their report based on N_2 isotherms and SEM data. The sample no. 7 particle is smooth and spherical and did not show a hysteresis loop for textural porosity in the N_2 isotherm, while sample no. 10, with a high hysteresis loop in 0.8-1.0 P/P_o, had an amorphous and rough surface. This characteristic between morphology and nanoporosity was the same as that of the MA sample. Therefore, the solidity and roughness of particles were dependent on the existence of textural porosity.

The difference in nanoporosity with particle morphology could be confirmed by TEM analysis (Fig. 2). For MA-1 (Fig. 2a), since

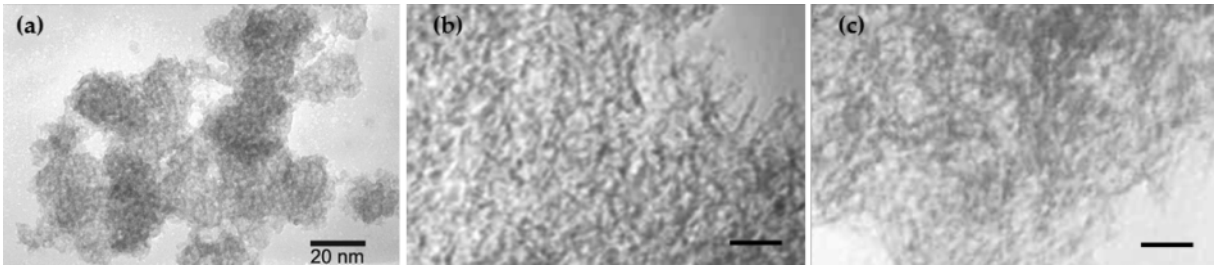

Fig. 2. TEM images of (a) MA-1, (b) MA-2, and (c) MA-3.

Table 1. Pore properties of mesoporous aluminas

Sample	$[H_2O]/[Al(Bu^sO)_3]$	Pore size/nm	FWHM of PSD[a]/nm	Surface area/m^2g^{-1}	Pore volume/cm^3g^{-1}
MA-1	48	7.7	2.9	386	1.0
MA-2	8	3.5	1.0	485	0.5
MA-3	4	3.5	1.4	420	0.6

[a]Full width at half maximum of pore size distribution.

the primary particle, with a diameter of 20-40 nm, forms aggregates, the void fraction between the aggregates formed textural pores and a coarse surface as shown in the SEM image (Fig. 1a). In the case of MA-2 and MA-3, the pores were wormhole or sponge-like in appearance, indicating the advantage of a highly inter-connected pore system.

The pore properties of the MA prepared are summarized in Table 1. As shown in the SEM and TEM results, MA-1 showed a large pore size, which was a textural pore induced by the aggregation of small primary particles. The excess water used in the preparation of MA-1 made the concentration of template diluted, and inhibited the formation of a condensed structure. To complete the hydrolysis of the aluminum alkoxide used, approximately 1.5 molar ratio of water/aluminum precursor is required. When an appropriate amount of water was used, as in the case of MA-2 and MA-3, the pore size distribution was found to be very narrow, and the surface area increased, as opposed to MA-1. For the stoichiometric ratio, the pore size remained the same due to the chemical template, while the surface area (264 m^2/g) and pore volume (0.2 cm^3/g) decreased dramatically. The ratio satisfied the minimal requirement for hydrolysis, which restricted the complete condensation of precursor and the complete mixing of micelles.

The crystalline phase of calcined MA was confirmed by ^{27}Al MAS NMR analysis. Typical active alumina used in industrial applications is γ- and η-alumina, generally known as spinel aluminas because their structures are very closely related to that of an Mg spinel. The XRD patterns of both active aluminas are similar, and it is not easy to distinguish the phase. Therefore, the coordination of Al atoms to the active alumina was investigated by ^{27}Al MAS NMR. As shown in Fig. 3, 4 and 6-coordinated Al atoms were found to be present. The ratio of Al^{VI} to Al^{IV} for calcined MA-2 was 2.6. The percentage of 4-coordinated Al present is reported to be 75±4% Al^{VI} in γ-alumina and 65±4% Al^{VI} in η-alumina [8,16]. Namely, the Al^{VI}/Al^{IV} value is 2.4-3.8 in γ-alumina and 1.6-2.3 in η-alumina. Therefore, the MA-2 alumina in this study is γ-alumina.

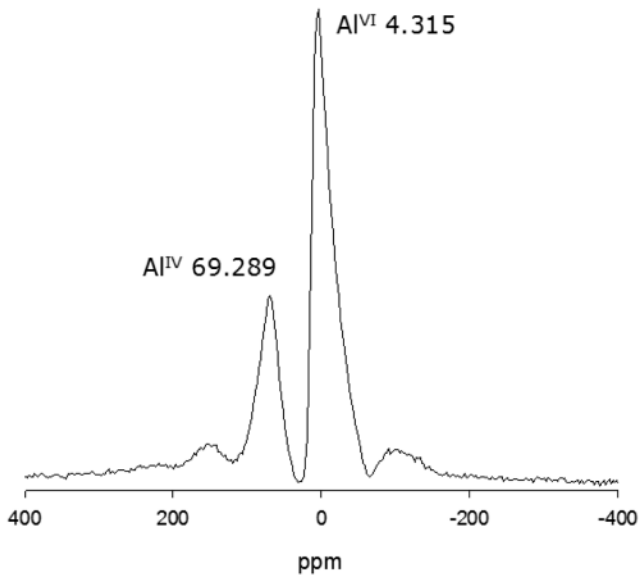

Fig. 3. ^{27}Al MAS NMR patterns of MA-2.

In conclusion, we report here on the effect of framework or textural nanoporosity on the bulk morphology of mesoporous aluminas. MA-1 with a well-developed framework porosity showed a solidified smooth surface, while MA-2 with a well-developed textural porosity had a coarse and aggregated morphology. MA-3 with both framework and textural porosity has features similar to both MA-1 and MA-2. The framework and textural porosity were induced by the template and aggregates of primary particle, respectively. Based on SEM, TEM, and N_2 isotherms, it should be noted that the nanoporosity of MA is correlated on the bulk surface morphology.

ACKNOWLEDGMENT

We are grateful to the Basic Research Program (R01-2006-000-10239-0) of the Korea Science & Engineering Foundation for financial support. This research was conducted through the Realistic 3D-IT Research Program of Kwangwoon University under the National Fund from the Ministry of Education and Human Resources Development (2006).

REFERENCES

1. Y. Kim, C. Kim, I. Choi, S. Rengaraj and J. Yi, *Environ. Sci. Technol.*, **38**, 924 (2004).
2. S. Rengaraj, Y. Kim, C. K. Joo and J. Yi, *J. Colloid Interf. Sci.*, **273**, 14 (2004).
3. P. Kim, H. Kim, Y. Kim, I. K. Song and J. Yi, *Appl. Catal. A*, **272**, 157 (2004).
4. P. Kim, J. B. Joo, H. Kim, W. Y. Kim, I. K. Song and J. Yi, *Catal. Lett.*, **104**, 181 (2005).
5. Y. Kim, B. Lee and J. Yi, *Korean J. Chem. Eng.*, **19**, 908 (2002).
6. C. Kim, Y. Kim, P. Kim and J. Yi, *Korean J. Chem. Eng.*, **20**, 1142 (2003).
7. Y. Kim, P. Kim, C. Kim and J. Yi, *Korean J. Chem. Eng.*, **22**, 321 (2005).
8. Y. Kim, C. Kim, P. Kim and J. Yi, *J. Non-Crystal. Solids*, **351**, 550 (2005).
9. Y. Kim, P. Kim, C. Kim and J. Yi, *J. Mater. Chem.*, **13**, 2353 (2003).
10. C. J. Brinker and G. W. Scherer, *Sol-gel science*, Academic Press (1990).

11. Y. Kim, B. Lee and J. Yi, *Separ. Sci. Technol*., **39**, 1427 (2004).
12. L. Mericier and T. J. Pinnavaia, *Adv. Mater*., **9**, 500 (1997).
13. M. Mesa, L. Sierra, J. Patarin and J.-L. Guth, *Solid State Sci*., **7**, 990 (2005).
14. M. Grun, K. K. Unger, A. Matsumoto and K. Tsutsumi, *Micropor. Mesopor. Mater*., **27**, 207 (1999).
15. P. T. Tanev and T. J. Pinnavaia, *Chem. Mater*., **8**, 2068 (1996).
16. L. J. Alvarez, A. L. Bumenfeld and J. J. Fripiat, *J. Chem. Phys*., **108**, 1724 (1998).